LUND UNIVERSITY

Measured Diversity Gains from MIMO Antenna Selection

Almers, Peter; Santos, Telmo; Tufvesson, Fredrik; Molisch, Andreas; Kåredal, Johan; Johansson, Anders J

Published in:
[Host publication title missing]

DOI:
10.1109/VTCF.2006.74

2006

Measured Diversity Gains from MIMO Antenna Selection

Peter Almers[1], Telmo Santos[1], Fredrik Tufvesson[1], Andreas F. Molisch[1,2], Johan Karedal[1] and Anders J Johansson[1]
[1] Dept. of Electroscience, Lund University, Box 118, SE-221 00 Lund, Sweden
[2] Mitsubishi Electric Research Labs, 201 Broadway, Cambridge, MA 02139, USA
Email: (Telmo.Santos@gmail.com and) Firstname.Lastname@es.lth.se.

***Abstract*— We investigate the diversity gain of MIMO systems with antenna selection in *measured* propagation channels for Wireless Personal Area Networks. We measure both the communication from an access point to a laptop, and between two handheld devices. Both the transmitter and receiver use antenna selection for diversity transmission and reception. We consider a closed-loop system where the transmitter has full channel state information, and analyze a number of different antenna selection algorithms and signal combining methods. We find that line of sight (LOS) and non-line of sight (NLOS) situations have fairly similar behavior, and that different polarizations result in similar SNR gains. We also find that RF-preprocessing of the signals is less effective for the hand held devices scenario than for the access point and laptop scenario. Finally, we compare bulk selection (same antenna subset is used for all frequency sub-channels) to per-tone selection (different antenna subsets can be used for each frequency sub-channel) for a wideband channel.**

I. Introduction

Wireless systems with multiple antennas at both the receiver (RX) and the transmitter (TX) side have been shown to offer great performance enhancement and hence attracted huge attention [1], [2]. Those so called multiple-input multiple-output (MIMO) systems exploit the multiple antennas to improve the data rate and/or the signal-to-noise ratio (SNR) of the system. The main disadvantage when deploying MIMO systems is the increased hardware complexity. While the required additional antenna elements themselves do not increase transceiver costs significantly, conventional MIMO systems require also one downconversion/upconversion (RF) chain for each antenna element; these RF chains are the most significant cost factor in most MIMO systems.

Antenna selection schemes, often called hybrid selection (HS), offer the possibility to reduce this hardware complexity and cost at a relatively small loss in performance [3]. In HS schemes, only the signals belonging to a *subset* of antenna elements are chosen for upconversion/downconversion and processing, hence the number of chains can be reduced. The selected antennas could be used for diversity and/or spatial multiplexing. In this paper, we focus on the use of MIMO for diversity, and furthermore assume that the TX has full channel state information and performs optimum *linear* weighting of a single transmit data stream; in other words, no space-time coding is considered.[1]

Due to their attractive properties, MIMO systems with antenna selection have been investigated extensively in the literature; for an overview see [5], [6], [7] and references therein. Furthermore, antenna selection has been included in the recent IEEE 802.11n standard draft [8] for high-throughput wireless computer networks, and antenna selection performance has been evaluated in that context. However, most of those investigations have been based on simplified theoretical channel models, including the independent identically distributed (i.i.d.) complex Gaussian channel and the 802.11n Kronecker channel model [9], often in combination with the assumption of uniform linear arrays. These investigations give valuable insights in the fundamental behavior of antenna selection schemes. However, they do not allow to assess the performance in realistic situations where irregular antenna structures, shadowing by the casing on which the antennas are mounted, or body shadowing by a user, play an important role.

In this paper we investigate the performance of eight different antenna selection schemes in *measured* WPAN channels[2]. We study an indoor office environment for both access point-to-PC/laptop (AP-PC) communication at 2.6 GHz and handheld-to-handheld (HH-HH) communication at 5.2 GHz. We present results for the flat-fading SNR gains for AP-PC and HH-HH communications in LOS and NLOS scenarios. We further investigate the polarization effect on SNR gain, and for frequency selective channels we compare the effect of per-tone selection and bulk selection schemes for different bandwidths.

II. System Model

For the analysis we consider a multiple antenna system with N_R receive and N_T transmit antenna elements from which a subset of L_R receive elements and L_T transmit elements is chosen; we use the short notation: $N_\mathrm{R} : L_\mathrm{R} \times N_\mathrm{T} : L_\mathrm{T}$. Maximum-ratio combining (MRC) and maximum-ratio transmission (MRT) are used for the selected antenna elements at receiver and transmitter, respectively. For the analysis we assume a quasi-static and flat fading channel. The channel between the selected antenna elements is described by the transfer matrix $\widetilde{\mathbf{H}} \in \mathbb{C}^{L_\mathrm{R} \times L_\mathrm{T}}$, which is a $L_\mathrm{R} \times L_\mathrm{T}$ sized sub-matrix of the full channel matrix $\mathbf{H} \in \mathbb{C}^{N_\mathrm{R} \times N_\mathrm{T}}$. Thus, the receive-transmit relation can be modelled as

$$\mathbf{r} = \widetilde{\mathbf{H}}\mathbf{v}s + \mathbf{n}, \tag{1}$$

[1]Theoretical aspects of antenna selection with space-time coding are discussed, e.g., in [4].

[2]Our recent paper [10] describes the propagation characteristics of these *channels*; however, no analysis of antenna selection and diversity schemes was performed there.

1-4244-0063-5/06/$20.00 ©2006 IEEE

where $\mathbf{r} \in \mathbb{C}^{L_{\mathrm{R}} \times 1}$ is the received vector, and $\mathbf{v} \in \mathbb{C}^{L_{\mathrm{T}} \times 1}$ is the transmit weighting vector. The noise vector $\mathbf{n} \in \mathbb{C}^{L_{\mathrm{R}} \times 1}$ is assumed to have an i.i.d. complex Gaussian distribution. Note that in this system model, the transmit data s is a scalar, i.e., we transmit only a single data stream. This stream might have been encoded with a forward error-correcting code, but there is no space-time coding. This approach is advantageous when the TX has full channel state information, as might occur, e.g., in a time-division duplex system, or a frequency-division duplex with explicit feedback [11]. At the RX side, the signal from the selected antenna elements is downconverted, weighted and combined with the receive weighting vector $\mathbf{u}^{\dagger}$. The optimal TX and RX weighting vectors (in SNR sense) $\mathbf{v}$ and $\mathbf{u}^{\dagger}$ are found from singular value decomposition of the channel transfer matrix $\widetilde{\mathbf{H}} = \mathbf{U}\Sigma\mathbf{V}^{\dagger}$, where $\mathbf{U}$ and $\mathbf{V}^{\dagger}$ are unitary matrices representing the left and right singular vector spaces, and Σ is a diagonal matrix containing all the singular values. Further, $[\cdot]^{\dagger}$ denotes the Hermitian transpose, and $\lambda_{\tilde{\mathbf{H}},i}$ denotes the $i-$th largest *singular* value of $\widetilde{\mathbf{H}}$. The optimum weight vectors are therefore the singular vectors belonging to $\lambda_{\tilde{\mathbf{H}},1}$, i.e., $\mathbf{v}_{\tilde{\mathbf{H}},1}$ and $\mathbf{u}^{\dagger}_{\tilde{\mathbf{H}},1}$, resulting in MRT and MRC.

The performance enhancement of the system utilizing diversity can be divided into two categories: (i) increased mean link gain due to beamforming at both RX and TX (resulting in a mean SNR gain of $N_{\mathrm{R}} \cdot N_{\mathrm{T}}$ in a pure LOS scenario), and (ii) diversity gain due to a change of the slope of the bit error rate (BER) vs. SNR curve; this diversity gain depends on the considered level of the BER (or outage). For a NLOS situation, the diversity order is equal to the number of independent TX/RX elements $N_{\mathrm{R}} \cdot N_{\mathrm{T}}$. We define the *total* diversity gain (at a specified outage level) as the decrease in SNR that is required for a multi-antenna system to achieve the same bit error rate as a single-antenna system [12].

III. Antenna Selections Schemes

As mentioned in the introduction, there are several selection schemes and pre-processing methods proposed in the literature. Furthermore, the optimum antenna elements can be selected in different ways. In the following, we list the algorithms that we compare in this paper.

A. Full-Complexity (FC)

All available antenna elements are used and the normalized SNR becomes [13], [14]

$$\gamma_{\mathrm{FC}} = \frac{\left|\mathbf{u}^{\dagger}_{\mathbf{H},1}\mathbf{H}\mathbf{v}_{\mathbf{H},1}\right|^2}{\left\|\mathbf{u}^{\dagger}_{\mathbf{H},1}\right\|^2} = \lambda^2_{\mathbf{H},1}. \tag{2}$$

The FC scheme results in full diversity order (e.g. $N_{\mathrm{R}} \cdot N_{\mathrm{T}}$ in the i.i.d. case) in addition to beamforming gain.

B. Hybrid Selection (HS)

1) Optimum Hybrid Selection (HS-B): A subset of antenna elements are selected and used for further processing. The only way to select the optimal antenna subset is an exhaustive search of all possible subset and pick the one giving the *best* SNR, though good approximate algorithms are known ([7] and references therein). Hence, HS-B at both link ends requires $\binom{N_{\mathrm{R}}}{L_{\mathrm{R}}} \cdot \binom{N_{\mathrm{T}}}{L_{\mathrm{T}}}$ computations for each channel realization. The normalized SNR of the *best* possible subset is [11], $\gamma_{\text{HS-B}} = \max_{\mathbf{S}\in\mathbf{S}_L} \lambda_{\mathbf{SH},1}$,where $\mathbf{S}$ is a selection matrix and $\mathbf{S}_L$ is the all possible selection sets.

2) Power Based Selection (PBS): In this case, the antennas are selected in a suboptimum approach. For the selection at the RX, we proceed the following way: First receive at one element and find the SNR that can be obtained with MRT at the transmitter. Then, receive at element two and again determine the SNR with MRT and so on. Choose the L best receive antennas as [11]

$$\mathbf{S}_{\mathrm{R}} = \arg\max_{\mathbf{S}\in\mathbf{S}_L} \left\|\mathbf{S}\mathbf{H}\mathbf{u}^{\dagger}_{\mathbf{H},1}\right\|_{\mathrm{F}}. \tag{3}$$

Selection at the transmitter is done in an analogous way. The resulting normalized SNR of $\gamma_{\mathrm{PBS}} = \lambda_{\mathbf{S}_{\mathrm{R}}\mathbf{H}\mathbf{S}_{\mathrm{T}},1}$.

3) Random and Worst Selection (HS-R and HS-W): For comparison, *random* selection (HS-R) and *worst* selection (HS-W) are also considered. In HS-R the subset is chosen randomly from $\mathbf{S}_L$, and in HS-W the worst of all possible subsets is selected from $\mathbf{S}_L$ as a worst case scenario.

C. Phase Shift Pre-processing and Selection (PSS)

In order to improve the beamforming gain, a pre-processing of the received signals can be performed in the RF domain, i.e., between the antenna elements and the selection switch [15]. The PSS pre-processing approach uses only variable phase shifters operating in the RF domain whose values are adjusted depending on the channel state information, but no variable-gain amplifiers. The scheme shows full diversity for *two* or more demodulators (PSS opt), i.e., identical performance compared to the FC scheme. The normalized SNR becomes $\gamma_{\text{PSS opt}} = \gamma_{\mathrm{FC}}$.For *one* demodulator (PSS sopt) the normalized SNR is

$$\gamma_{\text{PSS sopt}} = \frac{\left|\phi\mathbf{H}\mathbf{v}_{\mathbf{H},1}\right|^2}{N_{\mathrm{R}}},$$

where the applied phase shift ϕ is a simple sub-optimal solution for the optimal vector $\mathbf{u}_{\mathbf{H},1}$, including only the phase information of the entries in $\mathbf{u}_{\mathbf{H},1}$. PSS sopt is equivalent to equal gain combining [16].

D. FFT Pre-Processing and Selection (FFTS)

The FFT preprocessing can be viewed as a special case of the PSS, where the preprocessing matrix is a Butler matrix (FFT-matrix, Φ_{FFT}). Thus, the signal is Fourier transformed before down conversion and selection, see e.g., [17]. Note that the values of the phase shifters in the Bulter matrix are time-invariant and cannot be adjusted according to the channel state. The FFT pre-processing scheme works well for uniform linear arrays and highly correlated channels. The normalized SNR becomes, $\gamma_{\mathrm{FFTS}} = \max_{\mathbf{S}\in\mathbf{S}_L} \lambda_{\mathbf{S}\Phi_{\mathrm{FFT}}\mathbf{H},1}$.

IV. MEASUREMENT SETUP

For the performance analysis we use measurements in an AP-PC scenario at 2.6 GHz and HH-HH scenario at 5.2 GHz (in [10] the AP was referred to as ”fixed device”). The measurements were performed with the RUSK LUND channel sounder, and the total available bandwidth of 200 MHz was divided into 321 frequency points (sub-channels). The length of the test signal, as well as the guard period between successive test signals, was set to 1.6 μs corresponding to an resolvable excess delay of 480 m, which was enough to avoid significant inter-symbol interference between the transmitted test signals. Due to the short distances measured, and the high dynamic range of the measurement equipment, all measurement results showed a very high dynamic range and an SNR above 20 dB.

The access point was a dual-polarized $(4 \times 8 \times 2)$ $(\text{rows} \times \text{columns} \times \text{polarizations})$ patch array, see Fig. 2a. During the measurements, only the middle two rows $(2 \times 8 \times 2)$ were used, and all unused elements were terminated with 50 Ω-terminations. The AP array was tripod-mounted at a height close to the ceiling in order to increase the resemblance with a real AP.

The PC had an $(1 \times 4 \times 2)$ array, consisting of the same sort of elements as the AP, mounted on the back of the ”screen”, with the broadside direction aiming in the opposite direction of the ”keyboard”, see Fig. 2b. Since the ”screen” is slightly tilted backwards (in order to represent a typical laptop pose), so is the antenna array.

Two identical handheld devices were used, each made of a metal box with 4 slot antennas. Two slot antennas are at the front of the box, perpendicular to each other, one is mounted at the top side, and one is at the right side of the box, see Fig. 2c.

The measurements were performed in an office environment in the E-building at LTH, Lund University, Sweden. The building is made of reinforced concrete covered with brick walls, and with gypsum wallboards separating the different offices. Two different TX-RX positions were used for AP-PC measurements and two TX-RX positions for HH-HH (one for LOS and one for NLOS). Regarding LOS measurements, in this paper, we define LOS as any measurement where there is a direct optical path between the TX and the RX devices *or* the persons holding the devices. Hence, LOS also includes cases where some or all antenna elements are obstructed by the device or by the person carrying the device.

Measurements for a number of different orientations of the PC and the HH were taken for each TX-RX position. The orientations are shown in Fig. 2. More details about the measurement setup can be found in [10] and [18]. For each orientation, the channel gains are normalized; i.e., we assume a certain average receive power, where the averaging is done over the whole frequency range and the small-scale movements of the devices.

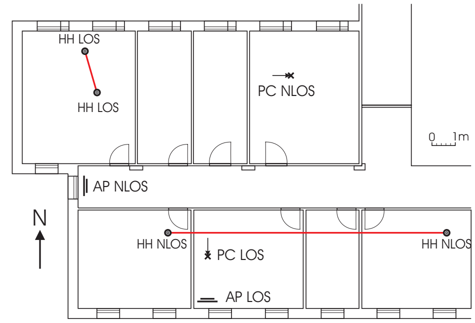

Fig. 1. Site map for the static AP-PC and HH-HH scenarios.

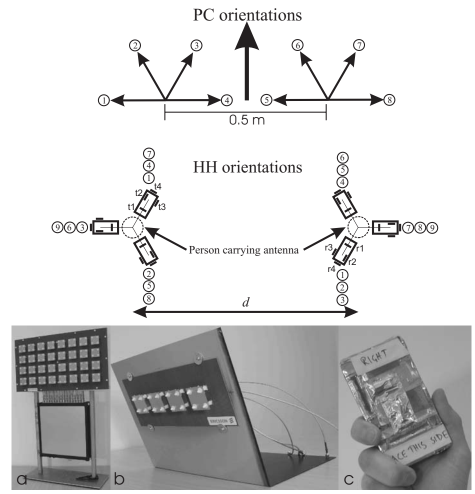

Fig. 2. Laptop (PC) and handheld (HH) orientations. The thick arrow is a reference also used in site map (see Fig. 1) for the PC. Pictures of: (a) AP, (b) PC and (c) one of the two identical HH devices.

V. RESULTS

A. $K-$factor Estimation

It is well known that the total diversity gain in a fading environment depends on the $K-$factor, which is the power ratio of the LOS and the scattered components of the channels [19]. For LOS, the gain is mainly due to an improvement of the average SNR gain, while in a NLOS scenario, gain due to the slope change of the BER-vs-SNR curve is the dominant mechanism.

We estimate the $K-$factor by the method of [20] for the different PC and HH orientations. For the AP-PC scenario the $K-$factor varies between $0.4 - 14$ and $0.2 - 1.1$ for LOS and NLOS, respectively (see [10] for further details). The relatively low $K-$factors in the LOS scenario are due to the orientation of the AP and PC (see Fig. 2); the elements on the tilted laptop 'screen' will sometimes not be exposed to the direct component. There is a notable difference of the $K-$factors between polarizations, i.e. horizontal polarization has a more pronounced LOS component than the vertical polarization, as a result of the differences in antenna patterns.

Notice that for the HH-HH scenario all elements can not simultaneously be exposed to the LOS component. Further

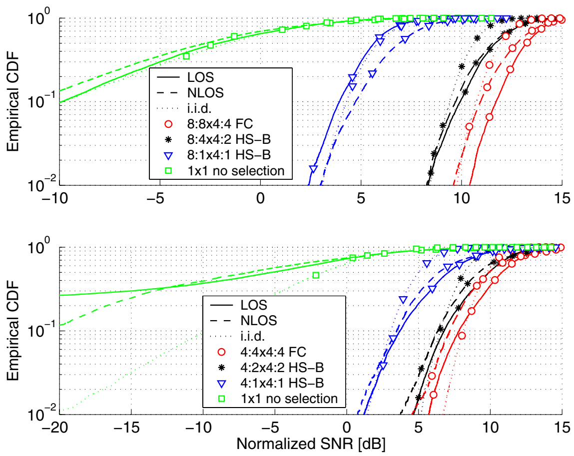

Fig. 3. Empirical CDFs of the normalized SNR for the AP-PC scenario in the upper subplot (rotation 2, 3, 5, 6 for LOS and rotation 3, 4, 6, 7 for NLOS) and HH-HH scenario in the lower subplot (rotation 1, 2, 4, 5 for LOS and rotation 9 for NLOS). Four schemes are used, all selecting the best element subset (HS-B), with respect to SNR, on both the TX and the RX side. Four dual polarized elements were used at the AP and two dual polarized elements were used at the PC. In addition the i.i.d. channel results are shown for comparison.

details of the statistical characteristics of the different elements can be found in [18].

B. HS-B Diversity

In this subsection, we investigate the performance of antenna selection, HS-B, compared to full complexity (FC) schemes for LOS, NLOS and a synthetic i.i.d channel. Both the AP-PC and HH-HH scenarios are considered. We evaluate the performance for a configuration where four dual-polarized elements are available at the AP and two dual-polarized elements are available at the PC, i.e., $N_\mathrm{R} = 8$, $N_\mathrm{T} = 4$.

In the upper subplot in Fig. 3 the cumulative distribution functions (CDFs) of the normalized SNR for AP-PC communication are presented. For the full-complexity scheme the LOS scenario shows a 1 dB higher gain than the NLOS scenario at an outage of 10%. We also find that the slope of the SNR CDF is very similar in the LOS, NLOS, and i.i.d. cases; note that the direct component sometimes is not that pronounced in the LOS case (see Sec. V-A). With a complexity reduction of 50%, i.e., when going from a 8×4 FC system (with $8+4 = 12$ RF chains) to $8 : 4 \times 4 : 2$ HS-B (with $4 + 2 = 6$ RF chains), the decrease of the total diversity gain is less than 2 dB at an outage of 10% for both the LOS and the NLOS scenarios. By selecting only one single element at both link ends (i.e., $8 : 1 \times 4 : 1$ HS-B) a complexity reduction of 83 % compared to FC is achieved, while the total diversity gain is reduced by about $5-8$ dB. However, at an outage of 10% the gain even for this extremely simple scheme is 15 dB for selection combining compared to no selection at all. It is also noteworthy that the diversity order of the FC and the different HS-B schemes is the same, confirming the theoretical prediction that the diversity order is retained by selection diversity [3].

In the lower subplot of Fig. 3 the CDFs of the normalized SNRs for the HH-HH scenario are presented. The HH devices have four single-polarized elements available. The difference in normalized SNR for the full complexity scheme between LOS and NLOS is about 0.5 dB, and a slightly steeper slope is noted for the LOS scenario compared to the NLOS. For the $4 : 2 \times 4 : 2$ HS-B results, LOS and NLOS preforms similarly. Also in this scenario the LOS component is not that pronounced since all elements cannot be in LOS simultaneously [10]. When going from FC to $4 : 2 \times 4 : 2$ HS-B, we reduce the RF complexity by 50%, while paying for this with a reduction of the total diversity gain by 1.5 dB at an outage of 10%. The diversity gain for selection combining compared to no selection at all is more than 25 dB at an outage of 10% for NLOS and more than 35 dB for LOS, due to the difference in average power between the HH elements resulting in large penalty when a bad element is selected. In the figure it can also be noted that the different elements of the HH device experience different propagation channels and attenuations [18], resulting in a SNR slope that is flatter compared to the i.i.d. channel. A general observation is that the diversity gain is not affected linearly, resulting in a better performance for the NLOS scenario compared to the LOS scenario for HS-B.

In Fig. 4 horizontal (H), vertical (V) and dual polarized (DP) configurations are compared for the HS-B and the FC scheme. As mentioned in the Sec. II the performance enhancement of the system utilizing diversity can be divided into mean link gain and diversity gain. With HS-B the beamforming gain is decreased linearly compared to the FC system with fewer number of antenna elements used in the subset. For the FC in the lower subplot of Fig. 4 the LOS performs better for all configurations.

There is not a large difference between polarizations. Note, however, that - due to the normalization to a constant receive SNR - the differences in received power between the polarizations are not included. Further, an antenna configuration with the same physical size as V and H, but enabling both polarizations (i.e., 16×8) is also analyzed. When antenna selection with $8 : 4 \times 4 : 2$ HS-B is used, the dual-polarized configuration has a gain of about 1 dB compared to the vertical-polarized one in LOS, at an outage of 10%. There is a 2.5 dB gain when utilizing both polarizations in configuration (i.e., 16×8 antenna elements) compared to the small configuration case (i.e., 8×4 antenna elements) for the antenna selection.

C. Algorithm Comparison

For the full-complexity schemes (FC), the AP-PC scenario the AP-PC uses twice as many elements as the HH-HH and we could expect a 3 dB SNR gain. However, [14] MIMO systems can obtain full beamforming gain only for extremely low angular spread. This explains why there is a 2.5 dB gap (between AP-PC and HH-HH) for the LOS case, while there is only 2 dB gap for the NLOS scenario in Fig. 5.

For antenna selection with instantaneous preprocessing, our results confirm the theory that the PSS opt algorithm

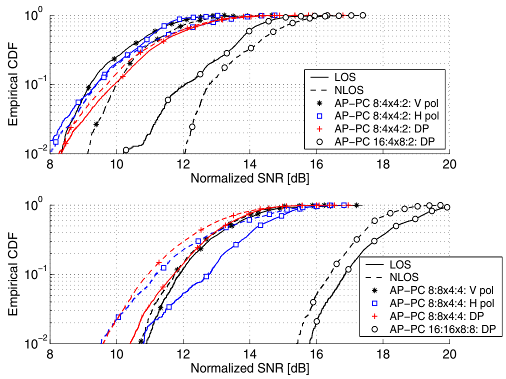

Fig. 4. Empirical CDFs of the normalized SNR for the AP-PC scenario. Two schemes are used: $8:4\times4:2$ and $16:4\times8:2$, all selecting the best element subset (HS-B), with respect to SNR, on both the TX and the RX side. Results from both dual polarized (DP) and single polarized (vertical and horizontal) configurations are presented for LOS (rotation 2, 3, 6, 7) and NLOS (rotation 3, 4, 7, 8).

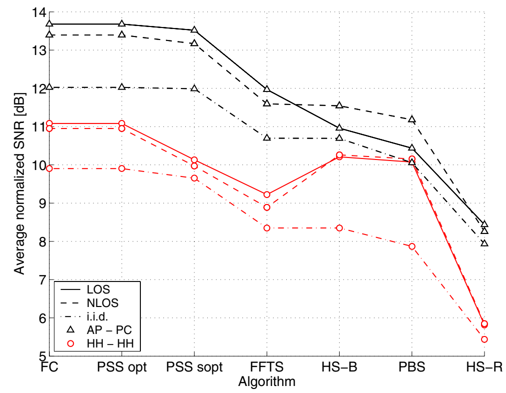

Fig. 5. The average normalized SNR for the different antenna selection schemes are presented. Both AP-PC ($8:4\times4:2$ vertical polarized elements) and HH-HH ($4:2\times4:2$) results are presented for LOS and NLOS. The same antenna selection algorithm was used at both ends. For comparison the i.i.d. channel results are presented.

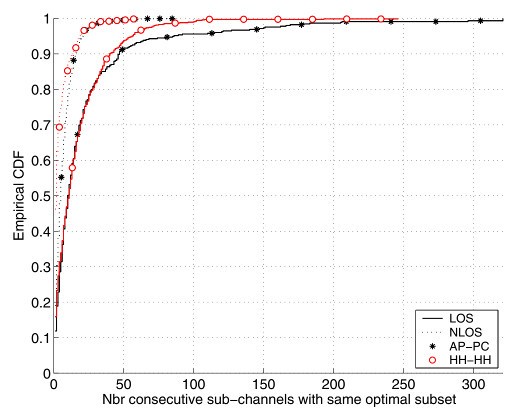

Fig. 6. CDFs of the number of consecutive sub-channels (out of the 321) that are using the same optimal subset for AP-PC ($8:4\times4:2$, DP) and HH-HH ($4:2\times4:2$). Both LOS and NLOS scenarios are considered.

performs equivalent to the full-complexity scheme [15]. The performance of the PSS sopt algorithm varies greatly. In the AP-PC scenario, the performance gap is negligible, while in the HH-HH case, it can be more than 1 dB.

Next, we compare the performance of the "standard" hybrid selection (HS-B) to the performance of the FFT-based selection. As predicted by theory, there is no difference in performance in i.i.d. channels. In the AP-PC scenario, we find an improvement by using the FFT of about 1 dB for LOS and no improvement for NLOS. For the HH-HH scenario, we find that the FFT considerably *decreases* the SNR, both for the LOS and the NLOS case. The reason for this effect are twofold: (i) the antennas on the handsets are not arranged in a linear form; therefore, the beampatterns formed by the FFT point into random directions; (ii) the average power received on the different antenna elements is unequal. Therefore, the spatial FFT pre-processing smears out the already concentrated power resulting in performance loss compared to no pre-processing (e.g., HS-B).

The large average power differences between the elements in the HH-HH scenario also results in a severe penalty when the good element(s) are not in the selected subset (compare HS-B and HS-R). Hence, the selection algorithm is more important for configurations with large average power differences between the elements. Even when picking the worst possible element subset in the AP-PC scenario the gains is at least 2 dB compared to a SISO system (this result is not shown in the figure for space reasons). Finally, we notice that power-based selection works well for almost all scenarios. Especially for the HH-HH case, power-based selection is almost optimum. This result was predicted for i.i.d. channels in [11]; it is actually more pronounced in our case, because the different antenna elements receive different average power.

D. HS-B Frequency Dependence

In this section, we investigate the performance of antenna selection used in a MIMO-OFDM system. Such a system is a more realistic scenario for broadband WLAN settings. In this scenario, the system model becomes frequency selective, i.e., Eq. (1) must be applied to each separate OFDM sub-channel.

We investigate two types of antenna selection: (i) bulk selection, where the bulk optimal antenna subset is used for *all* OFDM sub-channels; (ii) per-tone selection, where a different subset can be used for each tone. Naturally, the second solution requires a much higher complexity. It is however interesting to compare the relative performance differences between those cases.

In Fig. 6 the number of consecutive sub-channels that have selected the same optimal subset is shown. For the AP-PC setup $8:4\times4:2$ there are $\binom{8}{4}\cdot\binom{4}{2}=420$ available subsets and for HH-HH ($4:2\times4:2$) there are 36 available subsets. In agreement with intuition, the LOS scenarios (large coherence bandwidth) have few subset changes with frequency compared to NLOS. Note that for the AP-PC case there are some rotations where the same selection is used for all 321 sub-channels (200 MHz).

In Fig. 7 the CDFs of the normalized SNR averaged over

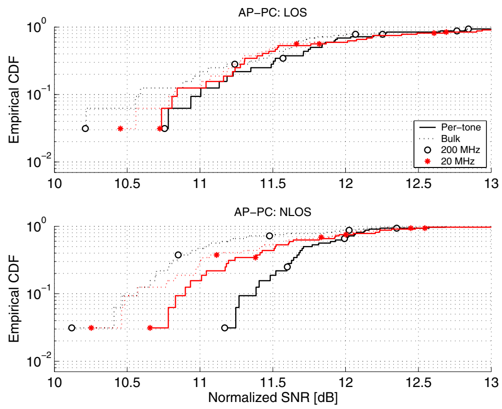

Fig. 7. The CDF of normalized SNR averaged over sub-channels (i.e. frequency diversity included) for the AP-PC ($8:4\times4:2$, DP) scenario. The antenna subset selection is either found per sub-channel (per-tone selection) or the same subset is used for all sub-channels (bulk selection). The frequency bandwidth is 20 MHz and 200 MHz.

the sub-channels within the selected bandwidth are presented for both bulk selection and tone-by-tone selection. AP-PC and HH-HH for both LOS and NLOS are considered. The results show, as expected, that (i) for a smaller bandwidth the bulk selection is closer to per-tone selection and that (ii) in a LOS scenario bulk selection, due to the smaller variations in used subsets, has a smaller performance loss (compared to per-tone selection) than for NLOS. Note also that the frequency selectivity results in a frequency diversity gain, hence the low variance of the normalized SNRs.

VI. Conclusions

We have performed an experimental evaluation of the closed-loop diversity gain that can be achieved by MIMO systems with antenna selection. Our evaluations were performed in WLAN and WPAN scenarios for AP-PC and HH-HH communication. Our main results can be summarized as follows:

- when reducing hardware complexity by 50% compared to a full-complexity system at both TX and RX, the reduction in diversity gain is between 1 and 2.5 dB.
- when reducing hardware complexity by more than 80%, i.e., to a single RF chain, the reduction in diversity gain is up to 5 dB.
- 35 dB diversity gain at an outage at 10% in HH-HH LOS scenario when selecting one element out of four.
- compact antenna arrays, using dual-polarized antennas provide the same diversity gain as more space-consuming single-polarized uniform linear arrays.
- for the analyzed WLAN and WPAN scenarios, FFT preprocessing in the RF domain resulted in moderate gains for AP-PC scenario, for the HH-HH scenario the FFT pre-processing performed worse than without pre-processing. PSS pre-processing results in performance that is equivalent to the full-complexity system when at least 2 RF chains are used.
- in MIMO-OFDM systems, the more practical bulk antenna selection provides a diversity gain that is only $1-1.5$ dB smaller compared to the theoretically optimum per-tone antenna selection, for the measured scenarios.

Our results thus confirm that antenna selection is a very attractive method for complexity reduction in MIMO systems with diversity.

VII. Acknowledgement

The authors would like to thank NEWCOM and Bristol University for making it possible for us perform measurements with their HH devices. This work was partly funded by an INGVAR grant of the Swedish Foundation for Strategic Research and a grant from Vetenskapsrådet.

References

[1] J. H. Winters, "On the capacity of radio communications systems with diversity in Rayleigh fading environments," *IEEE Journal on Selected Areas in Communications*, vol. 5, pp. 871–878, June 1987.
[2] G. J. Foschini and M. J. Gans, "On limits of wireless communications in fading environments when using multiple antennas," *Wireless Personal Communications*, vol. 6, pp. 311–335, 1998.
[3] M. Z. Win and J. H. Winters, "Analysis of hybrid selection/maximal-ratio combining in Rayleigh fading," *IEEE Transaction on Communications*, vol. 47, pp. 1773–1776, December 1999.
[4] D. A. Gore and A. J. Paulraj, "MIMO antenna subset selection with space-time coding," *IEEE Transactions on Signal Processing*, vol. 50, pp. 2580–2588, October 2002.
[5] A. F. Molisch and M. Z. Win, "MIMO systems with antenna selection," *IEEE Microwave Magazine*, vol. 5, pp. 46–56, March 2004.
[6] S. Sanayei and A. Nosratinia, "Antenna selection in MIMO systems," *IEEE Communications Magazine*, vol. 42, pp. 68–73, October 2004.
[7] N. B. Mehta and A. F. Molisch, "Antenna selection," in *MIMO antenna technology for wireless communications*, G. Tsoulos, Ed. Wiley, 2006, to appear.
[8] A. Stephens *et al.*, "Joint proposal–High throughput extension to the 802.11 standard: Mac," IEEE, Tech. Rep., January 2006.
[9] V. Erceg, L. Schumacher, P. Kyritsi, A. Molisch, and D. S. Baum *et al.*, "TGn channel models," *IEEE 802.11-03/940r2*, January 2004.
[10] A. Johansson, J. Karedal, F. Tufvesson, and A. F. Molisch, "MIMO channels measurements for personal area networks," in *Proc. Vehicular Technology Conference 2005 spring*, vol. 1. IEEE, May–June 2005, pp. 171–176.
[11] A. F. Molisch, M. Z. Win, and J. H. Winters, "Reduced-complexity transmit/receive-diversity systems," *IEEE Transactions on Signal Processing*, vol. 51, pp. 2729–2738, November 2003.
[12] A. F. Molisch, *Wireless communications*, 1st ed. IEEE Press: Wiley, 2005.
[13] T. K. Y. Lo, "Maximum ratio transmission," *IEEE Transactions on Communications*, vol. 47, pp. 1458–1461, October 1999.
[14] J. B. Andersen, "Antenna arrays in mobile communications: Gain, diversity, and channel capacity," *IEEE Antennas Propagation Magazine*, pp. 12–16, April 2000.
[15] X. Zhang, A. F. Molisch, and S.-Y. Kung, "Variable-phase-shift-based RF-baseband codesign for MIMO antenna selection," *IEEE Transactions on Signal Processing*, vol. 53, pp. 4091–4103, November 2005.
[16] R. Vaughan and J. B. Andersen, *Channels, propagation and antennas for mobile communications*, 1st ed. London, UK: IEE, 2003.
[17] A. F. Molisch and X. Zhang, "FFT-based hybrid antenna selection schemes for spatially correlated mimo channels," *IEEE Communications Letters*, vol. 8, pp. 36–38, January 2004.
[18] J. Karedal, A. J. Johansson, F. Tufvesson, and A. F. Molisch, "Characterization of MIMO channels for handheld devices in personal area networks," in *European Signal Processing Conference 2006*, Florence – Italy, September 2006, invited paper.
[19] M. Pätzold, *Mobile Fading Channles*. England: Wiley, 2002.
[20] L. J. Greenstein, D. G. Michelson, and C. Erceg, "Moment-method estimation of the Ricean K-factor," *IEEE Communications Letters*, vol. 3, pp. 175–176, June 1999.